Electronic Supplementary Material (ESI) for Nanoscale.

Supplementary Information

Small Iron Oxide Nanoparticles as MRI T_1 Contrast Agent: Scalable Inexpensive Water-Based Synthesis Using a Flow Reactor

Maximilian O. Besenhard,[a] Luca Panariello,[a] Céline Kiefer,[b] Alec P. LaGrow,[c] Liudmyla Storozhuk,[d] Francis Perton,[b] Sylvie Begin,[b] Damien Mertz,[b] Nguyen Thi Kim Thanh,[d,e,*] Asterios Gavriilidis[a,*]

[a] *Department of Chemical Engineering, University College London, London, WC1E 7JE, U.K.*
[b] *Institut de Physique et Chimie des Matériaux de Strasbourg, BP 43, 67034, Strasbourg, France*
[c] *International Iberian Nanotechnology Laboratory, Braga 4715-330, Portugal*
[d] *Biophysics group, Department of Physics and Astronomy, University College London, London, WC1E 6BT, U.K.*
[e] *UCL Healthcare Bio magnetic and Nanomaterials Laboratories, 21 Albemarle Street, London, W1S 4BS, U.K.*

* Corresponding authors: a.gavriilidis@ucl.ac.uk and ntk.thanh@ucl.ac.uk

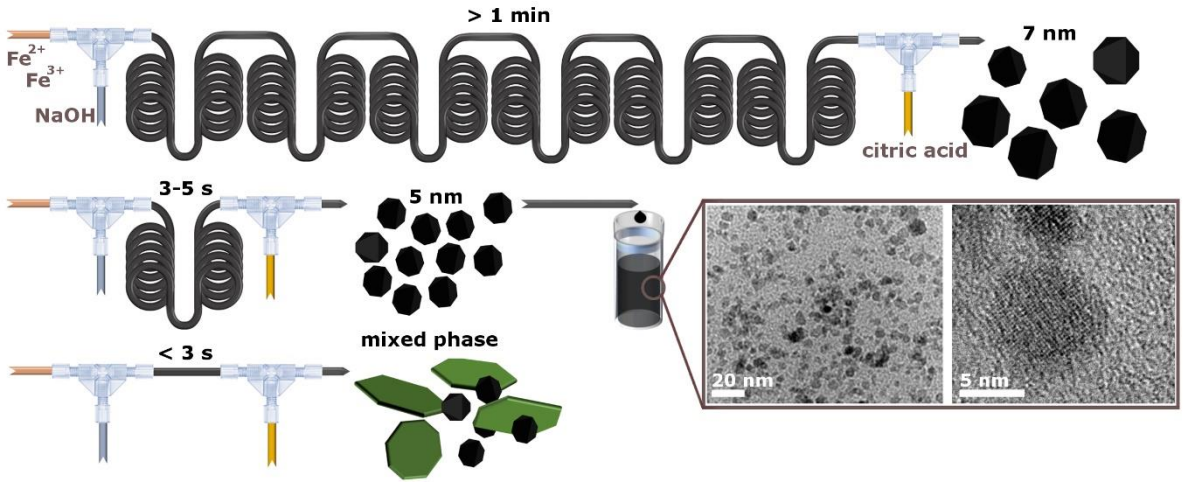

Contents:

SI1 Chemicals and components used for flow syntheses experiments

All chemicals used for this work are listed in Table S1. The components of the flow reactor used are listed in Table S2. Further details of the reactor such as tubing lengths and curvatures are provided in the supporting information of our previous study (Besenhard ***et al.***, *Chemical Engineering Journal*, 2020, 399, 125740). Note that the reactors used were not identical to our previous study and varied between the experiments, ***i.e.***, the tubing lengths between the first T-mixer and the second T-mixer in which the citric acid were altered.

Table S1: Details of chemicals used

Compound	Purchased from	Manufacturer	Product Nr.
Iron(II) chloride tetrahydrate, $FeCl_2 \cdot 4H2O$, ≥ 99 %	Sigma-Aldrich UK	Honeywell/Fluka	44939
Iron(III) chloride hexahydrate, $FeCl_3 \cdot 6H2O$, ≥ 99 %	Sigma-Aldrich UK	Honeywell/Fluka	31232
NaOH 2 M solution	Fischer Scientific Ltd	Honeywell/Fluka	35254
Citric acid (CA), $C_6H_8O_7$, 99 %	Sigma-Aldrich UK	Sigma-Aldrich	C0759
Dextran from *Leuconostoc spp.*, MW ~6,000	Sigma Aldrich UK	Sigma Life Science	31388
1.0 M HCl solution	Fischer Scientific	Honeywell/Fluka	15654940

Table S2: Details of reactor components used

Compound	Details	Material	Product Nr./manufacturer
Syringe pump	Each pump can fit 2 syringes		Legato210, KD Scientific
Syringes 100 ml	For precursor and NaOH solution	Glass	009760 (SGE syringes, TRAJAN)
Syringes 50 ml	For CA solution	Glass	009760 (SGE syringes, TRAJAN)
Tubing (used before CA addition)	1.0 mm inner diameter, 1.6 mm outer diameter	Polytetrafluoroethylene (PTFE)	JR-T-6807-M25 (VICI Jour)
Tubing (used after CA addition)	1.5 mm inner diameter, 2.5 mm outer diameter	Polytetrafluoroethylene (PTFE)	Z609730 (Sigma Aldrich)
1st T-mixer	0.5 mm channel diameter	Ethylenetetrafluoroethylene (ETFE)	P-632 (IDEX Health Science)
2nd T-mixer	0.5 mm channel diameter	Polyetheretherketone (PEEK)	P-716 (IDEX Health Science)
Water bath 1	Crystallisation dish 75 mm height, 140 mm diameter	Glass (Duran®)	216-1867 (VWR)
Magnetic stirrer and heater	ETS-D5 temperature controller		C-MAG HS 7 (IKA)
Water bath 2	Crystallisation dish 90 mm height, 190 mm diameter	Glass (Duran®)	216-1868 (VWR)
Magnetic stirrer and heater	ETS-D5 temperature controller		C-MAG HS 10 (IKA)

SI2 Additional XRD and TEM analysis

Figure S1 shows the XRD spectra of the particles synthesised with dextran in the precursor solution and quenching performed 5 s after initiating co-precipitation with a citric acid solution at 1.7 ml/min.

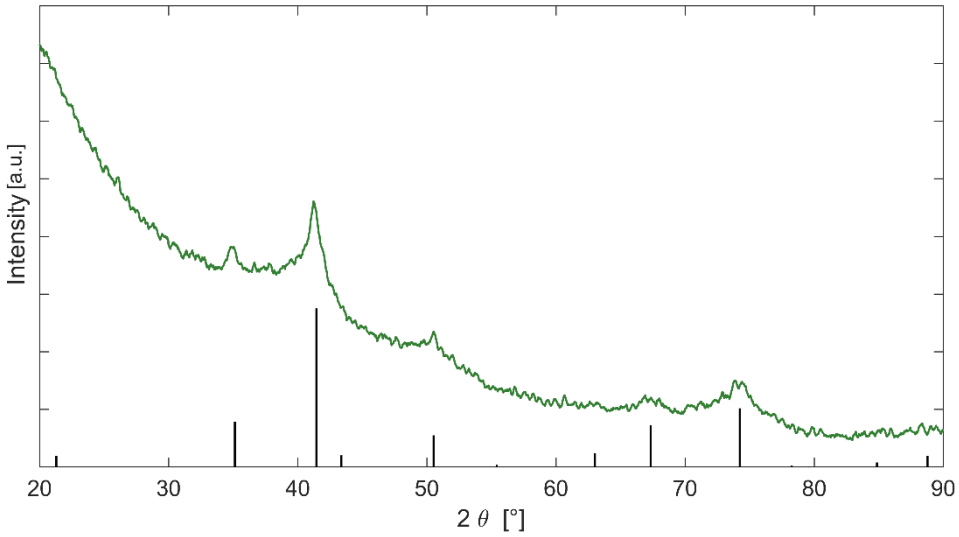

Figure S1: XRD pattern of IONPs synthesised with dextran in the precursor solution and quenching performed 5 s after initiating co-precipitation by feeding a 0.32 M citric acid solution at 1.7 ml/min (all at the standard reaction temperature of 60 °C). The black bars at the bottom are the reference pattern for magnetite (PDF ref. 03-065-3107)

Figure S2 shows the same XRD pattern as shown in Figure 3a but including also the pattern obtained from particles synthesised with quenching time 100 s, to allow for a better comparison. The XRD patterns show that the peaks assigned to magnetite become sharper (narrower full width at half maximum) when quenching time increases, which agrees with the hypothesis that particles continue to grow if not quenched.

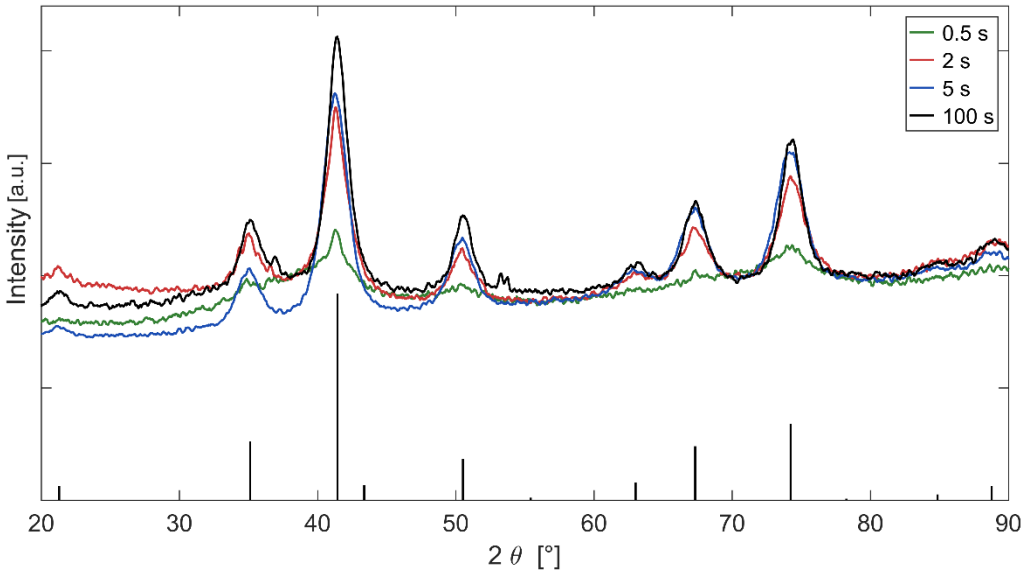

Figure S2: Overlaid XRD pattern of IONPs synthesised with quenching performed 0.5, 2 and 5 s (as shown in Figure 3a), and 100 s after initiating co-precipitation by feeding a 0.32 M citric acid solution at 2.1 ml/min (all at the standard reaction temperature of 60 °C). The black bars at the bottom are the reference pattern for magnetite (PDF ref. 03-065-3107).

Figure S3, Figure S4 and Figure S5 show the particle size distributions of the TEM analyses shown in Figure 3c, Figure 3e and Figure 4b.

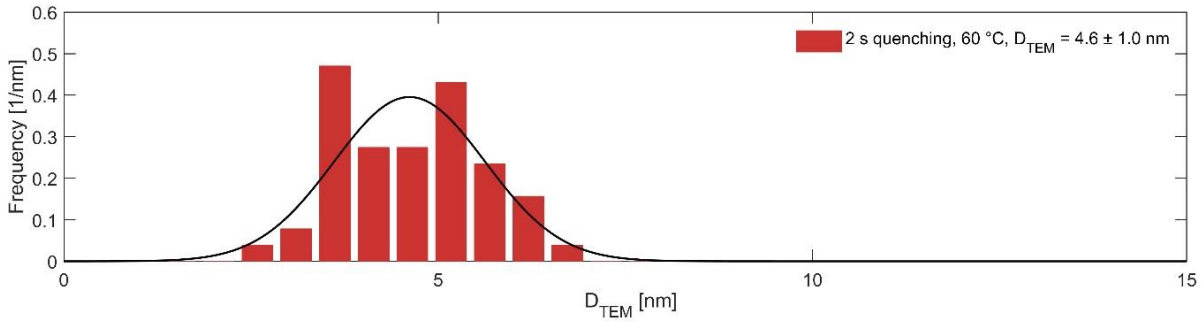

Figure S3: Particle size distributions obtained from TEM images of IONPs synthesised with quenching 2 s after initiating co-precipitation by feeding a 0.32 M citric acid solution at 2.1 ml/min and 60 °C (see Figure 3c$_{1\&2}$). The normal distribution (solid line) was generated using the mean particle size and the particle size standard deviation.

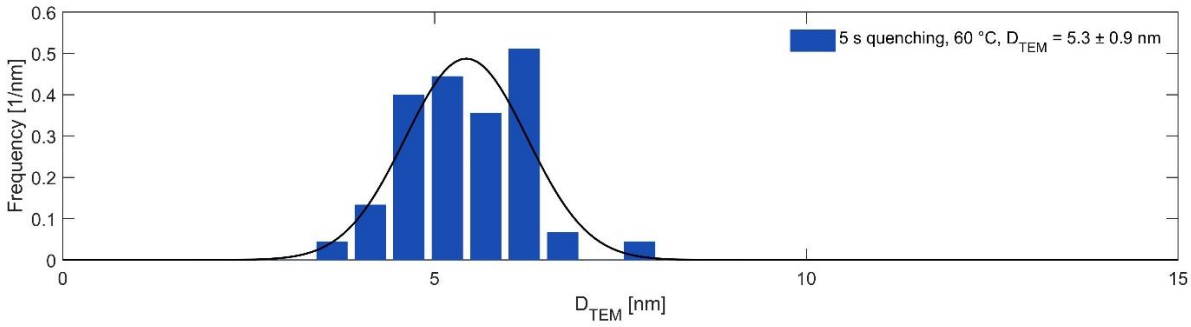

Figure S4: Particle size distributions obtained from TEM images of IONPs synthesised with quenching 5 s after initiating co-precipitation by feeding a 0.32 M citric acid solution at 2.1 ml/min and 60 °C (see Figure 3e$_{1\&2}$). The normal distribution (solid line) was generated using the mean particle size and the particle size standard deviation.

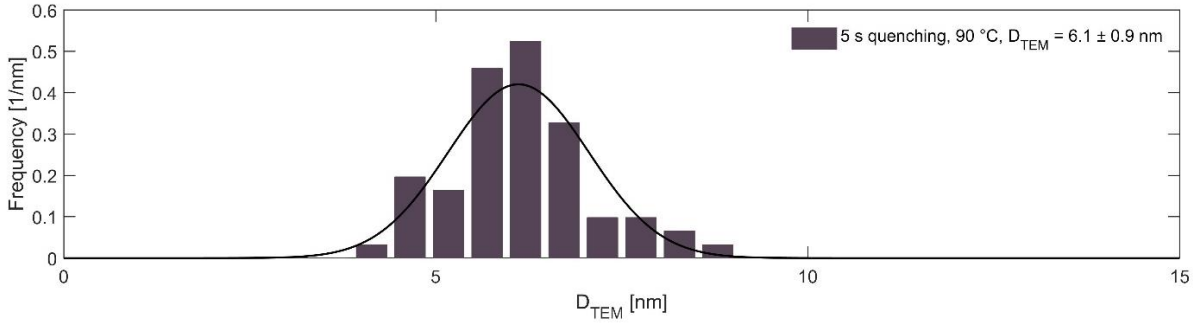

Figure S4: Particle size distributions obtained from TEM images of IONPs synthesised with quenching 5 s after initiating co-precipitation by feeding a 0.32 M citric acid solution at 2.1 ml/min and 90 °C (see Figure 4b$_{1\&2}$). The normal distribution (solid line) was generated using the mean particle size and the particle size standard deviation.

As citric acid can chelate iron and its effect on slowing down IONP growth has been reported, quenching was performed with a HCl solution for comparison. The synthetic procedure was identical to the one using CA solution, except that a 1 M HCl solution was fed at 1.9 ml/min instead. The washed and dried samples were analysed using a STADI P (STOE) goniometer equipped with a Mo Kα radiation source (λ = 0.07107 nm) operated at 30 mA and 5 kV. The XRD pattern of IONPs synthesised by quenching with HCl after 5 s and 100 s are shown in Figure S5. Similar to quenching with citric acid (see Figure S2), the peaks assigned to magnetite become sharper (narrower full width at half maximum) with increase of quenching time, which agrees with the hypothesis that particles continue to grow if not quenched.

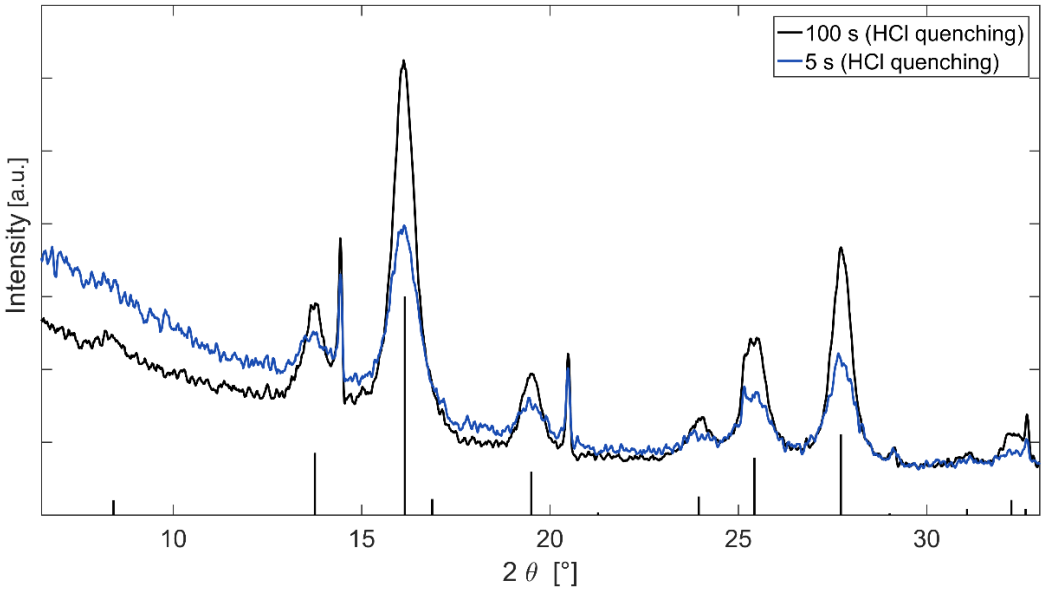

Figure S5: Overlaid XRD pattern of IONPs synthesised with quenching performed 5 s and 100 s after initiating co-precipitation by feeding a 1 M HCl solution at 1.9 ml/min (all at the standard reaction temperature of 60 °C). The black bars at the bottom are the reference pattern for magnetite (PDF ref. 03-065-3107). The sharp peaks around 2θ = 14.5°, 20.5°, and 32.5° match the pattern of NaCl, *i.e.*, residuals of sodium chloride formed during the synthesis using HCl and NaOH, which were not removed during washing.

SI3 TEM analysis of samples from repeated flow syntheses

Figure S7 shows TEM images of IONPs produced by repeating the synthesis with quenching 5 s after initiating co-precipitation *via* feeding citric acid solution at 2.1 ml/min. The obtained particle size D_{TEM} = 5.4 ± 0.8 nm was in good agreement with previous synthesis (D_{TEM} = 5.3 ± 0.9 nm, see Figure $3e_{1\text{-}2}$). The corresponding histograms from the TEM analysis is shown in the top of Figure S10.

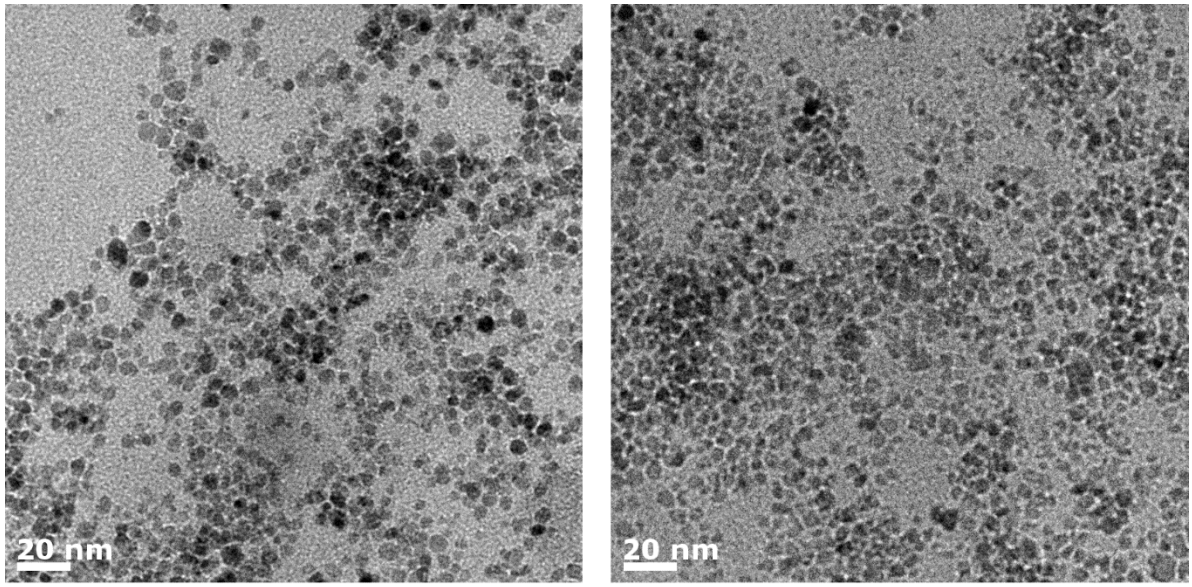

Figure S6: TEM images of IONPs synthesised with quenching 5 s after initiating co-precipitation by feeding a 0.32 M citric acid solution at 2.1 ml/min (all at the standard reaction temperature of 60 °C); D_{TEM} = 5.4 ± 0.8 nm (repeated synthesis and analysis).

Figure S8 shows TEM images of IONPs produced by repeating the synthesis with quenching 5 s after initiating co-precipitation *via* feeding citric acid solution at 1.9 ml/min, *i.e.*, feeding less citric acid solution. The obtained particle size D_{TEM} = 5.5 ± 1.0 was slightly, but not significantly, larger compared to IONPs quenched with 2.1 ml/min citric acid solution (based on an unpaired t-test with a 5 % significance level). The corresponding particle size distribution from the TEM analysis is shown in the middle of Figure S10.

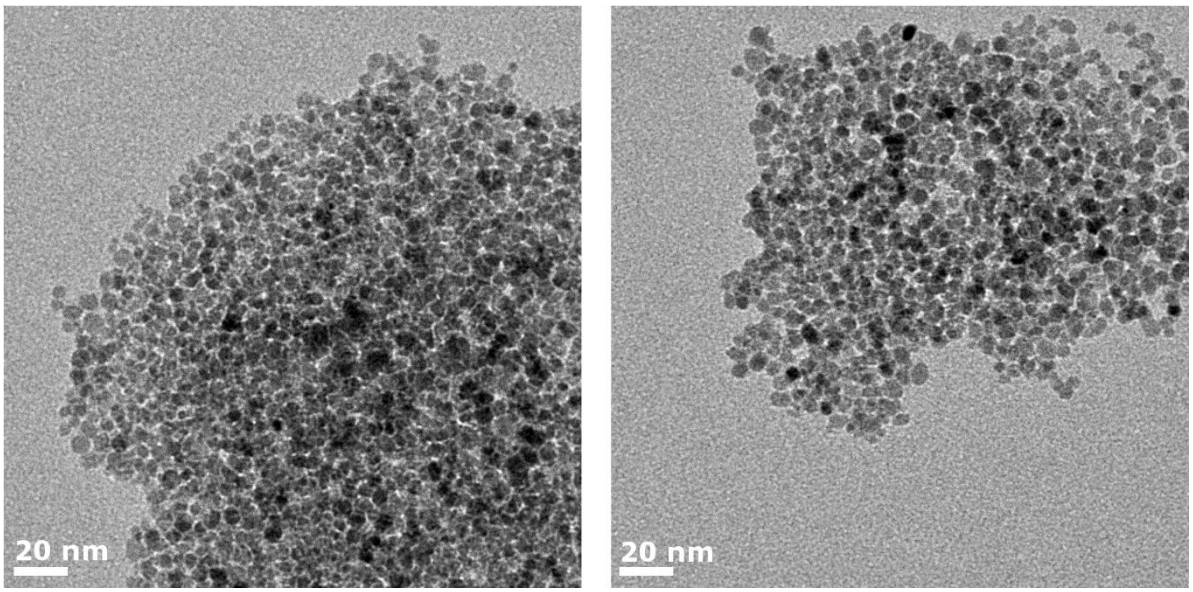

Figure S7: TEM images of IONPs synthesised with quenching 5 s after initiating co-precipitation by feeding a 0.32 M citric acid solution at 1.9 ml/min (all at the standard reaction temperature of 60 °C); D_{TEM} = 5.5 ± 1.0 nm (repeated synthesis and analysis).

Figure S9 shows TEM images of IONPs produced by repeating the synthesis with quenching 100 s after initiating co-precipitation *via* feeding citric acid solution at 2.1 ml/min, *i.e.*, the process previously described (Besenhard *et al*., *Chemical Engineering Journal*, 2020, 399, 125740*).* The corresponding particle size distribution from the TEM analysis is shown in the bottom of Figure S10. The obtained particle size D_{TEM} = 7.0 ± 1.0 is in good agreement with our previous study.

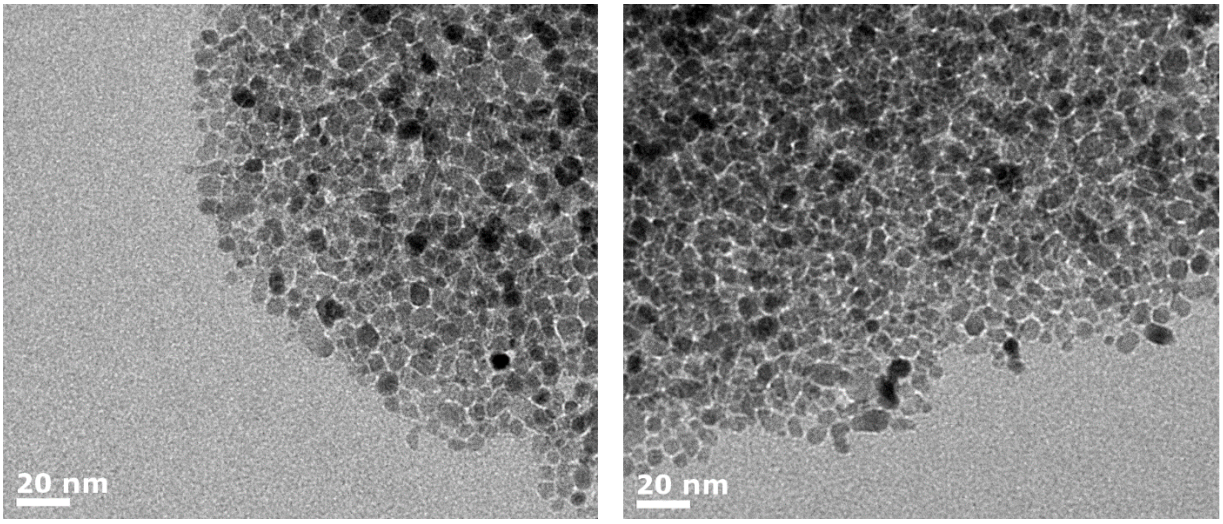

Figure S8: TEM images of IONPs synthesised with quenching 100 s after initiating co-precipitation (same procedure as in Besenhard *et al.*, *Chemical Engineering Journal*, 2020, 399, 125740) by feeding citric acid solution at 2.1 ml/min; D_{TEM} = 7.0 ± 1.0 nm (repeated synthesis and analysis).

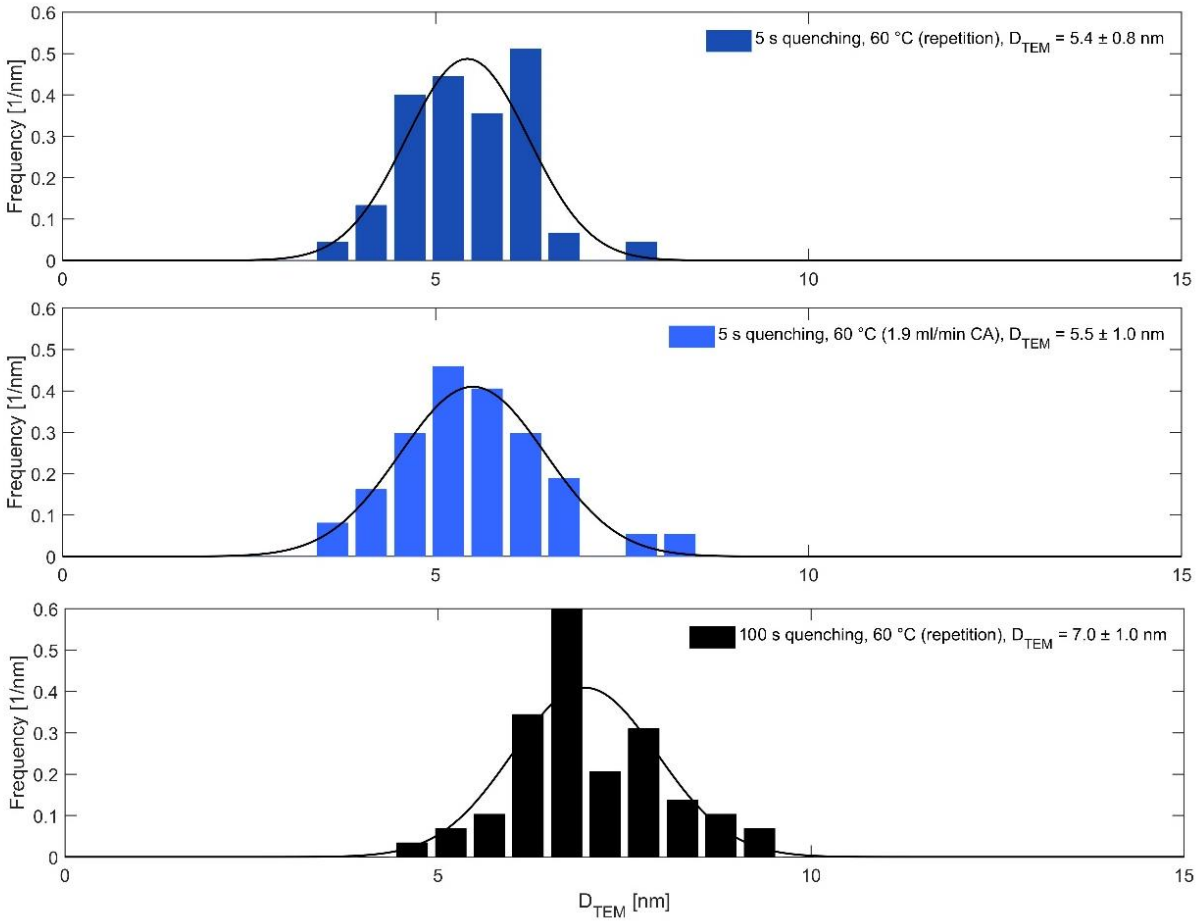

Figure S9: Particle size distributions obtained from TEM images of IONPs synthesised with quenching 5 s after initiating co-precipitation by feeding a 0.32 M citric acid solution at (*top*) 2.1 ml/min (repeated synthesis and analysis; see Figure S7) and (*middle*) 1.9 ml/min (see Figure S8). (*Bottom*) With quenching 100 s after initiating co-precipitation by feeding a 0.32 M citric acid solution at 2.1 ml/min (repeated synthesis from previous study; see Figure S9). The normal distributions (solid lines) were generated using the corresponding mean particle sizes and the particle size standard deviations.

SI4 SAXS studies

The SAXS curves of IONP solutions synthesised with different quenching times, at different temperatures, and in the presence of dextran are shown in Figure S11. For all SAXS curves, the background was corrected by subtracting the SAXS curve of water in a capillary of the same diameter (= the background) after merging the sample and water curve at the same transmission line. The radius of gyration R_g was determined *via* the Guinier approximation for globular particles (Equation S1) within a q range of q^2 = 0.097-0.203 nm^{-2} for all curves, see Table S3.

$$I(q) = I(0) \cdot \exp\left(-q^2 \cdot {R_g}^2/3\right) \qquad \text{Eq. S1}$$

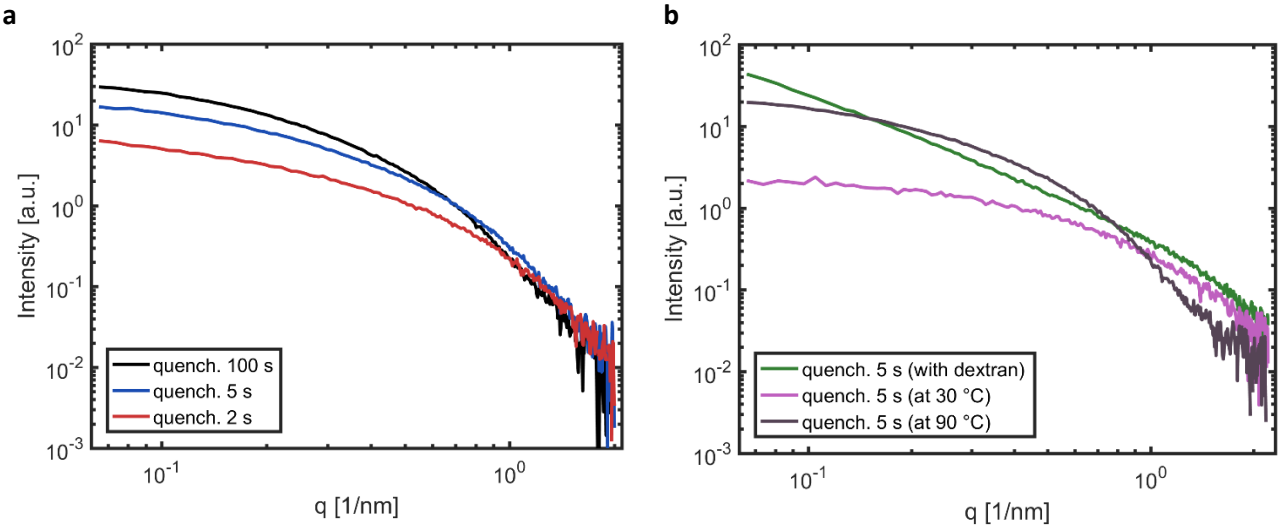

Figure S11 SAXS curves of IONP solutions synthesised; (**a**) at 60 °C (*i.e.*, the standard reaction temperature) with quenching performed 2, 5, and 100 s after initiating co-precipitation by feeding a 0.32 M citric acid solution at 2.1 ml/min (see SAXS measurements 1-3 in Table S3); (**b**) with quenching performed 5 s after initiating co-precipitation by feeding a 0.32 M citric acid solution at 2.1 ml/min and 90 °C (co-precipitation and quenching, aging was performed at 60 °C, see SAXS measurement 4 in Table S3), at 1.9 ml/min and 30 °C (co-precipitation and quenching, aging was performed at 60 °C; see SAXS measurement 5 in Table S3), and at 1.7 ml/min and 60 °C, but with dextran (see SAXS curve 6 in Table S3).

Table S3: SAXS characterisation summary of synthesised IONP solutions including the particle radius of gyration R_g and diameter assuming spherical particles D_{SAXS}.

IONP solution synthesised at:					
Co-precip. temp.	Quenching time	CA sol. flow rate	R_g	$D_{SAXS} = 2\ R_g \sqrt{5/3}$	SAXS curve
60 °C	100 s	2.1 ml/min	4.5 nm	11.6 nm	1
60 °C	5 s	2.1 ml/min	4.0 nm	10.3 nm	2
60 °C	2 s	2.1 ml/min	4.4 nm	11.4 nm	3
90 °C	5 s	2.1 ml/min	4.1 nm	10.6 nm	4
30 °C	5 s	1.9 ml/min	3.7 nm	9.6 nm	5
60 °C*	5 s	1.9 ml/min	4.2 nm	10.8 nm	6
* with dextran in the precursor solution					

The particle dimensions listed in Table S3 were estimated assuming monodisperse (and spherical) particles. Hence, the obtained dimensions should be considered with care, especially for samples that were shown to contain intermediate iron oxide phases, where TEM analysis revealed a high polydispersity.

SAXS curves are a representation of the distances between points with a change in electron density (e.g., at particle-solution interfaces). Short distances scatter towards large q values and larger distances towards

small q values. Although this is a drastic oversimplification, neglecting for example constructive and destructive interference, it allows for a rough comparison of SAXS curves. For example, the particles synthesised with dextran present in the precursor solution are likely highly aggregated/agglomerated, as the SAXS curve (green line in Figure 11b) follows a power law function (*i.e.*, linear increase in intensity towards small q values in the log-log plot)

$$I(q) \sim q^{\alpha} \qquad \text{Eq. S2}$$

where α is the slope of the decrease of the intensity related to the mass fractal dimension (see A. Guinier and G. Fournet, *Small Angle Scattering of X-Rays*, *Wiley Intersciences, New-York, 1955*).

Although the hydrodynamic diameter of IONPs synthesised at 30 °C and with a quenching time of 5 s (D_h = 55 nm), and 60 °C with a quenching time of 2 s (D_h = 29 nm) indicate the presence of large nanoparticles, the corresponding SAXS curves and radii of gyrations (pink line Figure b and red line Figure a, see SAXS measurements 5 and 3 in Table S3) do not exhibit indications for larger particles. This discrepancy can be explained by particles having a large translational diffusion coefficient (on which DLS analysis is based), but short distances between points with a change in electron density (on which SAXS analysis is based).

For example, plate like structures (as seen in the TEM analysis of the solution synthesised with quenching after 2 s, see Figure $3c_{2\text{-}3}$) as formed by green rust magnetite intermediates for co-precipitation syntheses, diffuse slowly through the solution (large translational diffusion coefficient) but have short distances between particle-solution interfaces (the plate diameter) determining the SAXS spectra.

For the other samples, the obtained D_{SAXS} is in fair agreement with the hydrodynamic diameter (which is expected to be slightly larger than D_{SAXS} since D_h accounts too for solvent molecules moving with the particles). As the IONP diameters obtained *via* TEM are of the same order of magnitude, this suggests a minimum level of agglomeration.

SI5 Normalisation of magnetisation hysteresis curves *via* TGA

Magnetisation hysteresis curves of dialysed and dried IONPs synthesised at 60 °C (*i.e.*, the standard reaction temperature) with quenching performed 5 s after initiating co-precipitation by feeding a 0.32 M citric acid solution at 2.1 ml/min are shown in Figure 3g. TGA was used for the normalisation of these hysteresis curves, *i.e.*, to report the mass magnetisation in emu per g Fe.

TGA revealed an IONP mass fraction of 0.7 (= 70 %, see Figure S12). This fraction had to be converted to the amount of g Fe per g sample. This was done by assuming the IONPs were magnetite (Fe_3O_4) and multiplying by the molecular weight (MW) ratio of magnetite and Fe accordingly. Hence, the mass magnetisation in emu per g Fe was obtained from the sample mass magnetisation in g per sample by Equation S3.

$$Mass\ magnetisation\ \left[\frac{emu}{g_{Fe}}\right] = Mass\ magnetisation\ \left[\frac{emu}{g_{sample}}\right] \cdot 1/0.7 \cdot \frac{MW_{magnetite}}{3 \cdot MW_{Fe}}. \qquad \text{Eq. S3}$$

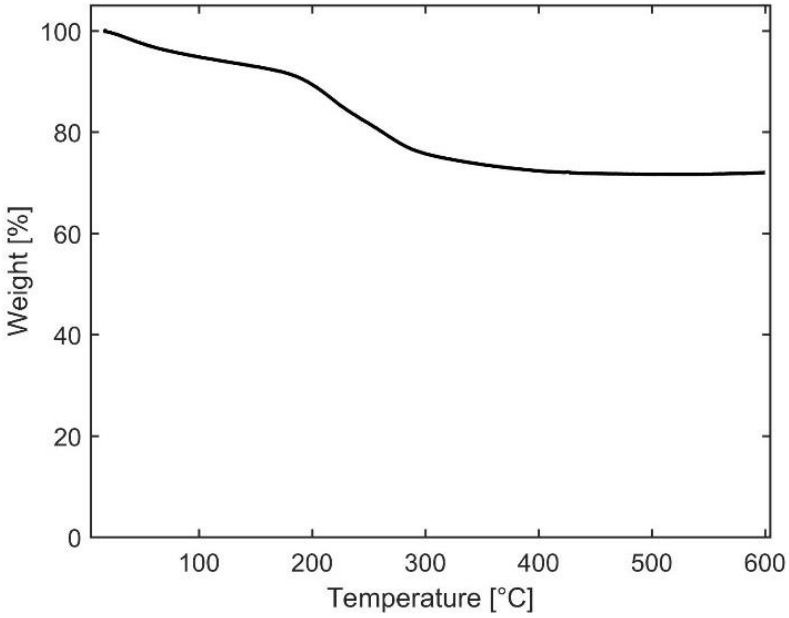

Figure S12: Thermogravimetric analysis of IONPs synthesised at 60 °C, *i.e.*, the standard reaction temperature, with quenching performed 5 s after initiating co-precipitation by feeding a 0.32 M citric acid solution at 2.1 ml/min

SI6 Comparison of batch and flow synthesis

A batch experiment was performed to test if the flow synthesis (with quenching after 5 s, see IONP flow synthesis with different quenching times) yields small IONPs when performed in batch. Batch reactors exhibit macromixing (or global mixing) times, *i.e.*, the time it takes after reagent addition till the concentration profile the reactor is homogeneous, in the order of seconds or minutes (see e.g. ***Houcine et al.***, *Effects of Stirred Tank's Design on Power Consumption and Mixing Time in Liquid Phase, Chem. Eng. Technol., 2000, 23, 605-613* and ***Kordas et al.***, *Study of Mixing Time in a Liquid Vessel with Rotating and Reciprocating Agitator, Ind. Eng. Chem. Res., 2013, 52, 13818-13828*). Both, smaller volumes and higher stirring rates (usually expressed in terms of the power input [W/kg], with limitations for large volumes) lead to faster mixing. This explains the difficulty to scale-up processes with fast reaction kinetics, hence, requiring fast mixing, because mixing times can hardly be kept short when increasing the reactor volume. This does also apply to our synthesis involving a rapid particle formation step after mixing the precursor and base solution and quenching particle growth by the precisely timed addition of a citric acid solution.

To allow for fast mixing also in batch, the batch synthesis was performed using small reaction volumes. 5 ml of precursor solution was kept at vigorous stirring in a 20 ml vessel immersed in a 60 °C water bath. Using 2 pipettes, 5 ml of the base solution was added first, followed 5 s later by the addition of 2.1 ml of the 0.32 M citric acid solution (replicating the flow synthesis with quenching after 5 s). Since i) the flow synthesis allowed to preheat the precursor and base solution to 60 °C before mixing (only the precursor solution was at kept 60 °C in batch), hence, co-precipitation occurred at well-defined temperatures, ii) mixing in batch is slower, iii) reagent addition is not immediate in batch (pipetting takes ~0.5 s), iv) and timing reagent addition as closely as in flow is challenging (± 0.5 s for manual pipetting), the batch synthesis cannot fully imitate the flow synthesis.

Figure S13 shows the TEM images of IONPs produced in batch (D_{TEM} = 4.8 ± 1.6 nm). The batch synthesis yielded a higher polydispersity compared to the corresponding flow synthesis and the particles were partly agglomerated (see Figure S14). This was attributed to the higher (compared to the flow synthesis) spatial inhomogeneity of temperature, pH, reagent concentrations, causing co-precipitation, quenching and stabilisation to happen at different conditions. Nevertheless, the batch synthesis also yielded small IONPs, but, despite the small reaction volumes used for this batch study, the polydispersity was higher. This shows that scale-up of this synthesis in batch is not trivial.

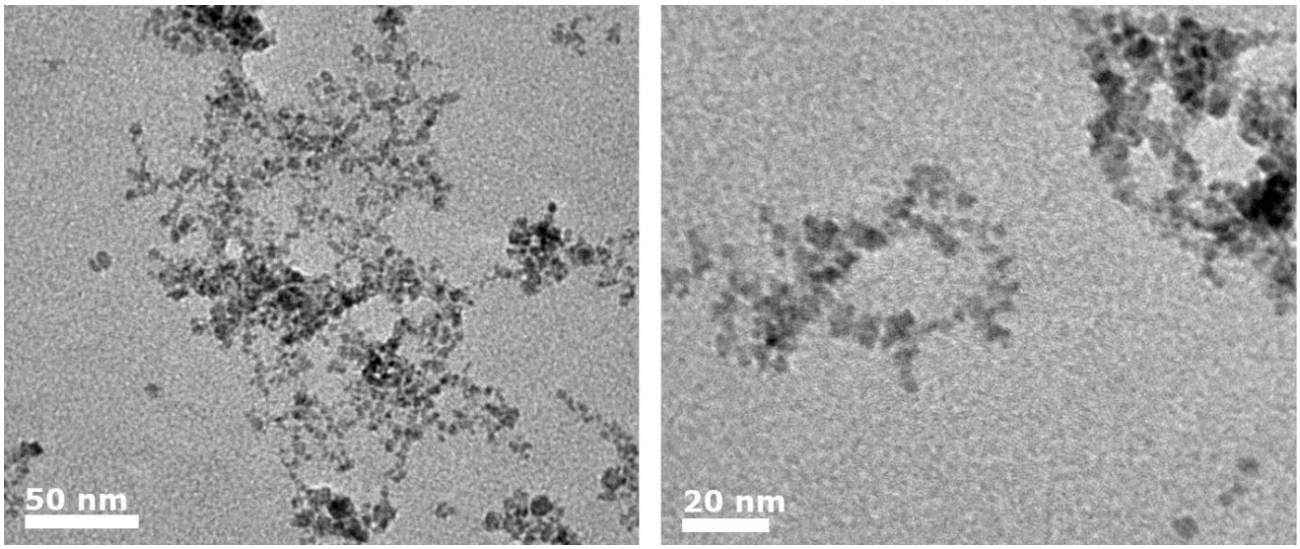

Figure S13: TEM images of IONPs synthesised in batch with quenching 5 s after initiating co-precipitation (i.e., after adding 5 ml of the base solution to the precursor solution stirred at 60 °C) by adding 2.1 ml of a 0.32 M citric acid solution; D_{TEM} = 4.8 ± 1.6 nm (repeated synthesis and analysis).

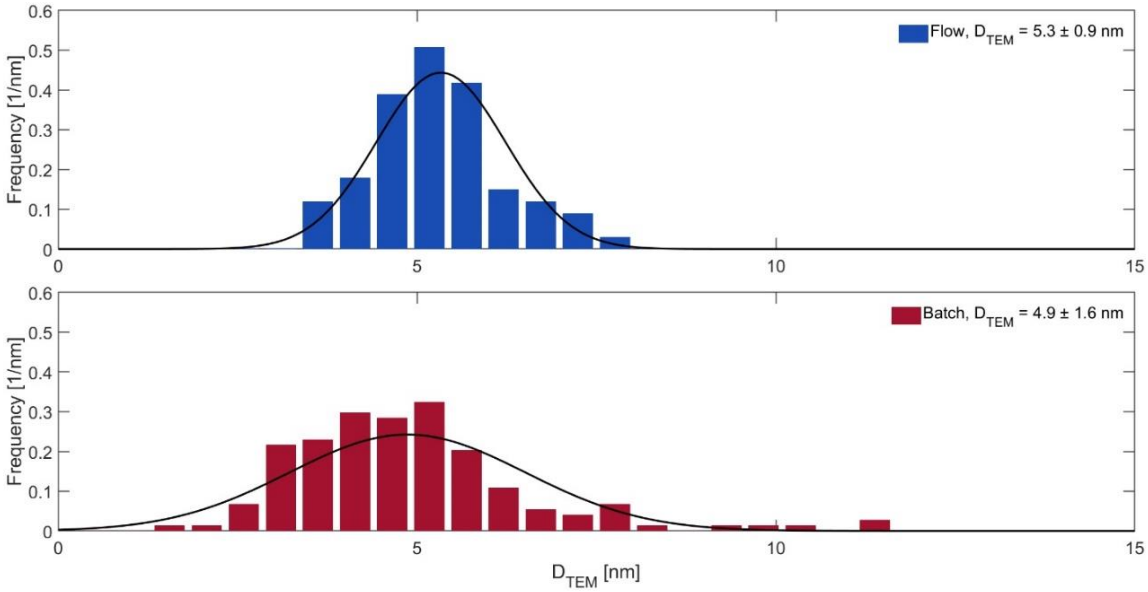

Figure S14: Particle size distributions obtained from TEM images of IONPs synthesised (*top*) in flow (= Figure S4) and (*bottom*) in batch (see Figure S13). The normal distributions (solid lines) were generated using the corresponding mean particle sizes and the particle size standard deviations.